Theoretical investigation of modulated currents in open nanostructures

Valeriu Moldoveanu,[1] Andrei Manolescu,[2] and Vidar Gudmundsson[3]
[1]*National Institute of Materials Physics, P.O. Box MG-7, Bucharest-Magurele, Romania*
[2]*School of Science and Engineering, Reykjavik University, Kringlan 1, 103 Reykjavik, Iceland*
[3]*Science Institute, University of Iceland, Dunhaga 3, IS-107 Reykjavik, Iceland*
(Received 3 September 2009; revised manuscript received 29 October 2009; published 25 November 2009)

We investigate theoretically the transport properties of a mesoscopic system driven by a sequence of rectangular pulses applied at the contact to the input (left) lead. The characteristics of the current which would be measured in the output (right) lead are discussed in relation with the spectral properties of the sample. The time-dependent currents are calculated via a generalized non-Markovian master equation scheme. We study the transient response of a quantum dot and of a narrow quantum wire. We show that the output response depends not only on the lead-sample coupling and on the length of the pulse but also on the states that propagate the input signal. We find that by increasing the bias window the new states available for transport induce additional structure in the relaxation current due to different dynamical tunneling processes. The delay of the output signal with respect to the input current in the case of the narrow quantum wire is associated to the transient time through the wire.

DOI: 10.1103/PhysRevB.80.205325 PACS number(s): 73.23.Hk, 85.35.Ds, 85.35.Be, 73.21.La

I. INTRODUCTION

Time-dependent transport measurements at the nanoscale provide important insight into the intrinsic properties of semiconductor structures such as relaxation and dephasing times[1] and play a crucial role in single-shot spin read-out schemes.[2] Consequently transient response of quantum structures to pulsed signals gains interest from experimental point of view. Recently Naser *et al.*[3] measured the time-dependent current through a quantum point contact when a pulse generator is coupled to the input lead. The output signal was measured for different amplitudes and rise times of the pulse. The decay of the output current was roughly exponential and it was suggested that such a device could be used as a microwave circuit element. In another recent experiment Lai *et al.*[4] performed transient current measurements for a Ge quantum dot when trapezoidal voltage pulses were applied to one electrode. The transient current mimics the pulse shape and the extracted time-dependent occupation number in the system follows an accumulation/depletion cycle.

From the theoretical point of view the transient currents have been calculated by various methods. Stefanucci *et al.*[5,6] combined the Keldysh formalism and the density-functional theory to study the response of a nanostructure to a time-dependent bias between the leads. In the partitioning approach the transient currents induced through a few-level quantum dot by a modulation of the contacts between the leads and the sample was calculated in Ref. 7 and a scattering theory of the time-dependent magnetotransport in a long quantum wire was proposed in Ref. 8.

These studies were essentially focused on understanding the transient regime and the onset of the steady state. Therefore the time-dependent driving used in the calculations did not describe pulsed signals, but rather an initial switching stage followed by a constant, time-independent value. In particular sudden coupling or smooth coupling lead to qualitatively different output signals. Another problem considered in the time-dependent transport calculations is the quantum pumping.[9–12] In this case one obtains averaged currents through an unbiased system which is perturbed by *two* time-dependent potentials oscillating out-of-phase.

In this work we discuss transport calculations for a mesoscopic sample driven out of equilibrium by both a constant bias applied between the leads and a fast oscillating signal applied at the contact between the lead and the sample. If the signal has a rectangular shape the setup is in some sense similar to the pump-and-probe configuration used in the transient spectroscopy experiments of Fujisawa *et al.*[1] The time-dependent signal was applied on the sample and the main aim was to extract the spin relaxation time by pushing *one* excited state into the transport window during the pulse.

Here we discuss the transient response of the system from a different angle: if a sequence of rectangular pulses that modulate the coupling to the left lead is viewed as an input signal then one can study the propagation of this signal trough the system and the corresponding current in the right (i.e., output) lead. Our problem is therefore closer to the experiments by Naser *et al.*[3] and Lai *et al.*[4] Besides the very ambitious goal of assembling quantum dot structures in complex mesoscopic circuits operating such as quantum gates we believe there is another important motivation for such a study. The transient response of the sample to the modulation of the contact is a consequence of the internal electron dynamics which depends crucially on the electronic states participating in transport. The point is that by changing the bias applied on the system one selects different states in the transport window and then the output current may carry important information about the electron dynamics in the sample. Even if the level structure of the sample may be known from other type of measurements, the tunneling rates associated to each quantum state or the propagation properties of the "orbitals" are not easily understood.

We aim at describing the following transport experiment through a mesoscopic structure: the contact between the sample and the left lead opens and closes periodically by applying rectangular pulses on the metallic gates that define the contact region. At the same time the contact between the

 ©2009 The American Physical Society

sample and the right lead gradually opens. Then each time the left contact closes the electrons in the sample can only escape into the right lead. These relaxation processes of various states in the sample depend mainly on the corresponding tunneling rates which in turn are given by the coupling of the states to the output contact. In real samples the states that participate in transport have different tunneling coefficients and therefore it is not obvious that the relaxation current follows a simple exponential decay. We show that the transient response of the sample is in general more complex. Sometimes the output current may look exponential, but often may also carry a fine structure reflecting the presence of several quantum states propagating through the sample and various relaxation processes corresponding to transitions between these states and the right lead.

A recent attempt to describe rectangular pulses in quantum dots was made by Oh *et al.*[13] Their sample model was a two-level quantum dot and for transport calculations they used rate equations with time-dependent tunneling coefficients. Instead, our calculations are done using the generalized non-Markovian master equation (GME) approach presented in one of our recent works.[14] We take into account the geometry of the system and its spectral properties which determine the tunneling coefficients and therefore the currents driven by the external bias. The generalized master equation method is well known from quantum optics.[15–17] The application of the GME method to quantum transport received attention only in the last years in the context of transient currents, measurement theory or full-counting statistics or coherent control of transport (see, e.g., Refs. 18–25).

The content of the paper is organized as follows: the formalism is briefly explained in Sec. II, the numerical simulations are reported in Sec. III, and the main conclusions are included in Sec. IV.

II. GENERALIZED MASTER EQUATION METHOD

In this section we introduce the Hamiltonian of the system, the underlying notations and we summarize the main equations derived in our previous work Ref. 14. We consider a mesoscopic system which is coupled to two leads at $t=0$ and described by the following second-quantized Hamiltonian (h.c. denotes Hermitian conjugation):

$$H(t) = \sum_{l=L,R} \int dq \varepsilon^l(q) c_{ql}^\dagger c_{ql} + \sum_n E_n d_n^\dagger d_n + \sum_{l=L,R} \sum_n \int dq \chi^l(t) (T_{qn}^l c_{ql}^\dagger d_n + \text{h.c.}), \quad (1)$$

where $c_{ql}^\dagger$, c_{ql}, and $d_n^\dagger$, d_n are creation and destruction operators for electrons with momentum q and energy $\varepsilon^l(q)$ in the lead l, and with energy E_n in the sample, respectively. The labels L and R denote the left and right lead. The second-quantized form of the Hamiltonian is constructed from the states ϕ_n of the isolated sample and from the generalized eigenfunctions ψ_q^l describing a semi-infinite lead. The third term is the tunneling Hamiltonian and contains the time-dependent switching functions $\chi^l(t)$ and the coupling matrix elements $T_{qn}^{L,R}$ associated to each pair of states $\{\psi_q^{L/R}, \phi_n\}$ from the leads and the sample. The pulses applied at the contact region between the left lead and the samples are simulated by the function χ_L which by construction has a rectangular shape. Although our formalism could also be implemented for a continuous model (see Ref. 26) here we use a lattice model for which the matrix elements are given by (see Ref. 14):

$$T_{qn}^l = V_l \psi_q^{l*}(0_l) \phi_n(i_l), \quad (2)$$

where V_l is the coupling strength between the lead l and the sample, 0_l is the site of the lead l which couples to the contact site i_l in the sample. The eigenfunctions of the sample ϕ_n and the corresponding energies E_n are numerically computed by diagonalizing the single-particle Hamiltonian of a two-dimensional lattice with N sites [see for example Eq. (1) from our previous work Ref. 14]. The generalized eigenfunctions of the semi-infinite lead ψ_q^l and its spectrum $\varepsilon^l(q)$ are known analytically:

$$\psi_q^l(m) = \frac{\sin[q(m+1)]}{\sqrt{\pi t_L \sin q}}, \quad \varepsilon^l(q) = 2t_L \cos q, \quad (3)$$

q being the momentum $[q \in (0, \pi)]$ and t_L the hopping constant on leads. We emphasize that even in this simple lattice model the coupling matrix elements introduced in Eq. (2) depend both on the energy and of the localization of the sample states. A similar model for the transfer Hamiltonian was proposed by Maddox *et al.*[27] We stress that while ψ_q^l and ϕ_n do not overlap the coupling T_{qn} is not vanishing. Moreover, our method goes beyond the wide band limit because the energy dependence is present through the q dependence of ψ_q and also through the eigenfunctions ϕ_n (i.e., states with different energies E_n have different coupling to the leads).

The statistical operator of the open quantum system is denoted by W and solves the Liouville equation: $i\dot{W}(t) = [H(t), W(t)]$, with the initial condition $W(t=0) = \rho_L \rho_R \rho_S$. This means that before the coupling the sample is described by the statistical operator ρ_S defined just below, and the leads are characterized by equilibrium distributions $\rho_{L,R}$ with different chemical potentials $\mu_L > \mu_R$.

The many-body states of the system are described by the sequence of occupation numbers of the single-particle states $\{\phi_n\}$ for the isolated system. We shall denote the many-body states by Greek letters, i.e., $|\nu\rangle = |i_1^\nu, i_2^\nu, \ldots, i_n^\nu \ldots\rangle$ and by i_n^ν the occupation number of the n-th single-particle state. If the initial state of the disconnected sample is $|\nu_0\rangle$ then $\rho_S = |\nu_0\rangle\langle\nu_0|$. For example, if two electrons are situated on the lowest levels at $t \le 0$ we have $|\nu_0\rangle = |110\ldots.\rangle$.

Following the main lines of the superoperator method[28,29] we take the partial trace of W over the Fock space of the leads and end up with a master equation for the reduced density operator $\rho(t) = \text{Tr}_L \text{Tr}_R W(t)$ with the initial condition $\rho(t=0) = \rho_S$ up to second order in the tunneling Hamiltonian:

$$\dot{\rho}(t) = -\frac{i}{\hbar}[H_S, \rho(t)] - \frac{1}{\hbar^2}\sum_{l=L,R}\int_0^\pi dq\chi^l(t)\{[\mathcal{T}_l, \Omega_{ql}(t)] + \text{h.c.}\}, \tag{4}$$

where we have introduced the operators (see Ref. 14 for details):

$$\Omega_{ql}(t) = e^{-itH_S}\int_{t_0}^{t} ds\chi^l(s)\Pi_{ql}(s)e^{i(s-t)\varepsilon^l(q)}e^{itH_S},$$

$$\Pi_{ql}(s) = e^{isH_S}[\mathcal{T}_l^\dagger\rho(s)(1-f^l) - \rho(s)\mathcal{T}_l^\dagger f^l]e^{-isH_S},$$

$$\mathcal{T}_l(q) = \sum_{\alpha,\beta}\mathcal{T}^l_{\alpha\beta}(q)|\alpha\rangle\langle\beta|,$$

$$\mathcal{T}^l_{\alpha\beta}(q) = \sum_n T^l_{nq}\langle\alpha|d_n^\dagger|\beta\rangle. \tag{5}$$

It is clear that $\mathcal{T}^l_{\alpha\beta}(q)$ describes the "absorption" of electrons from the leads to the system and changes the many-body states of the latter from β to α. Observe that $\mathcal{T}^l_{\alpha\beta}(q)\neq 0$ only if the number of electrons in the many-body states α and β differ by one. f_l denotes the Fermi function in the lead l. The difference between the chemical potentials defines the bias applied across the sample $eV=\mu_L-\mu_R$. Observe also the presence of loss and gain terms in Π_{ql}.

We also define a set of relevant states located in the energy window $[E_{\min}, E_{\max}]$, where $E_{\min}<\mu_R<\mu_L<E_{\max}$. This 'active' window includes only those states of the sample that are relevant to the transport. More precisely, $E_{\min}$ is chosen such that the levels with lower energy are fully occupied both prior to the coupling of the leads, i.e., for $t\leq 0$, and also after the coupling began, at $t>0$, in the presence of the bias. Similarly, $E_{\max}$ is selected such that all states with higher energy are permanently empty. Consequently the states outside this energy window do not contribute to the current. Based on this picture we conclude that it is sufficient to compute an "effective" reduced density matrix by taking into account only those many-body configurations resulting from the single-particle states within the active window. Also for the simplicity of notation we shall specify in the many-body states only the occupation numbers of the single-particle states within the active window. Of course, the validity of this truncation should be checked in the numerical simulations by gradually enlarging the active window $[E_{\min}, E_{\max}]$ until the calculated currents become stable.

In principle some of the levels above the bias window could contribute to the transient currents, if the corresponding coupling to the leads is high and if the amplitude of the time-dependent modulations is sufficiently large to allow tunneling to these levels. We have checked numerically that this is not the case for the results presented in Sec. III. On the other hand, the cotunneling processes which involve coherent tunneling of two electrons are known to be important at rather large coupling to the leads, which is not the case here. We also recall that the master equation is derived by taking into account only quadratic terms of H_T in the integrodifferential equation and as such describes only sequential tunneling.

The time evolution of the charge residing in the active region is related to the diagonal elements of the reduced density matrix:

$$\langle Q_S(t)\rangle = \sum_n\sum_\nu i_n^\nu\langle\nu|\rho(t)|\nu\rangle.$$

The continuity equation relates the rate of change in $\langle Q_S\rangle$ to the difference between the total currents in the two leads, i.e., $d\langle Q_S(t)\rangle/dt = J_L(t) - J_R(t)$. If the switching functions $\chi_{L,R}$ would be both smooth and approaching a constant, the system eventually evolves to a steady state where the identity $J_L=J_R$ holds. This is not the case here as $\chi_L\neq\chi_R$ and consequently the charge inside the sample varies. Using the GME, Eq. (4), one can easily identify the contribution of each level n to the currents in the left and right lead:

$$J_l = \sum_n J_{l,n},$$

$$J_{l,n} = -\frac{1}{\hbar^2}\sum_\nu i_n^\nu\int_0^\pi dq\chi^l(t)\langle\nu|[\mathcal{T}_l, \Omega_{ql}(t)] + \text{h.c.}|\nu\rangle, \tag{6}$$

where $i_n^\nu=0,1$ is the occupation number of the n-th single-particle state inside the active window. The sign of the net currents in the leads is positive if it is oriented from the left to the right, i.e., $J_L>0$ if the electrons flow from the left lead toward the sample and $J_R>0$ if they flow from the sample toward the right lead. During the transient regime the sign of the net currents may change in time.

The GME is numerically solved through the Crank-Nicolson method (see the details in Ref. 14). Throughout this work the Coulomb interaction effects are not considered; further discussion on this point is given at the end of Sec. III.

III. NUMERICAL RESULTS

The first system we consider is a rectangular two-dimensional lattice having 25×20 sites. The corresponding Hamiltonian has 500 eigenvalues E_n and eigenvectors ϕ_n, $n=1,2,\ldots,500$, as many as the number of sites. The energy unit is given by the hopping parameter in the sample $t_D=\hbar^2/2m^*a^2$, where a is the lattice constant and m^* is the electron effective mass in GaAs. The spectrum of the isolated sample is contained in the range $(-2t_D, 2t_D)$. For $a=8$ nm our lattice describes a 200 nm$\times$160 nm sample. We fix $kT=0.1$ meV which corresponds to a low temperature $T=1.15$ K. The sites of the system are denoted by i and are specified by the pair of coordinates (i_x, i_y).

In order to describe the gradual coupling of the leads to the sample and the periodic modulation of the left contact we define analytically the coupling functions $\chi_l(t)$. We want the coupling to the right lead to be established at $t=0$ and evolving smoothly to a constant value. As in our previous work we use a Fermi-like function $\chi_R=1-2f(t)$ where $f(t)=(e^{\gamma t}+1)^{-1}$ and the parameter γ defines the smoothness of the coupling. The rectangular pulses applied to the left lead have

a period $T=4(T_1-T_0)$, and are tailored from the functions $f(t)$ and $1-2f$ (T_0 and $T_1>T_0$ are two input parameters, k is the period index and we use the notation $t_k=kT$):

$$\chi_L(t)=\begin{cases}1-2f(t), & \text{if } t<T_0,\\ f(t-T_1-t_{k-1}),\\ \text{if } t\in\left[T_0+t_{k-1},T_0+t_{k-1}+\dfrac{T}{2}\right),\\ [1-2f(t-T_1-t_{k-1}-T/2)],\\ \text{if } t\in\left[T_0+t_{k-1}+\dfrac{T}{2},T_0+t_k\right).\end{cases} \tag{7}$$

Before $t=T_0$ the coupling to the leads increases smoothly from 0 and we take T_0 such that $\chi_{L,R}$ saturate before T_0. Note that around $t=T_1\chi_L$ decreases and then vanishes; the coupling is restored again around $t=T_1+T/2$. It is easy to see that the pulse length $\tau_p=T/2$. In the numerical simulations the pulse length τ_p is varied by changing the shift T_1 of the Fermi functions. As a consequence on the first period (i.e., $t\in[T_0,T_0+T]$) the function χ_L drops later for larger values of T_1.

We denote the pulse length by τ_p. We think this kind of time-dependent perturbation is a reasonable model of an experiment in which the sample is smoothly coupled to the leads with different chemical potentials, possibly reaching an equilibrium state before the pulses begin to act.

A problem related to the one we studied here was considered by Jauho *et al.*[30] in a pioneering work on time-dependent transport. The transient current through a resonant level calculated via the Green-Keldysh formalism in the presence of a rectangular bias shows a relaxation pattern after the pulse ends. Besides the more detailed description of the many-level structure and of the contacts, a major difference between the two models is that in our work the bias is constant, the time dependence comes from the modulation of the *contact* region between the leads and the sample, while in the work of Jauho *et al.* the spectrum of the leads becomes time-dependent. Transient calculations for a step-like bias were also reported by Stefanucci and Almbladh[5] in partition-free approach (see, e.g., Fig. 7 in their paper).

The currents depend strongly on the placement of the contacts. In this example the two leads are attached at diagonally opposite corners of the sample. We first choose the chemical potentials $\mu_L=-3.65$ and $\mu_R=-3.70$. Then our sample has nine energy levels below μ_R, and as we checked they do not contribute significantly to the transport. The chosen active region contains two states within the bias window which are E_{10} and E_{11} and two more states above μ_L, which are E_{12} and E_{13}. Instead of the label $n=10,11,12,13$ for the states in the active window (in the present example), we will also use the label $k=1,2,3,4$, respectively.

In Figs. 1(a)–1(d) we show the site occupation probabilities $|\phi_n(i)|^2$ for the active states. We emphasize that the middle state with $n=12$ or $k=3$, Fig. 1(c), is weakly coupled to the leads while the other ones have a larger, but still moderate coupling.

Figures 2(a)–2(c) show the time-dependent total currents in both leads for different pulse lengths. We also indicate

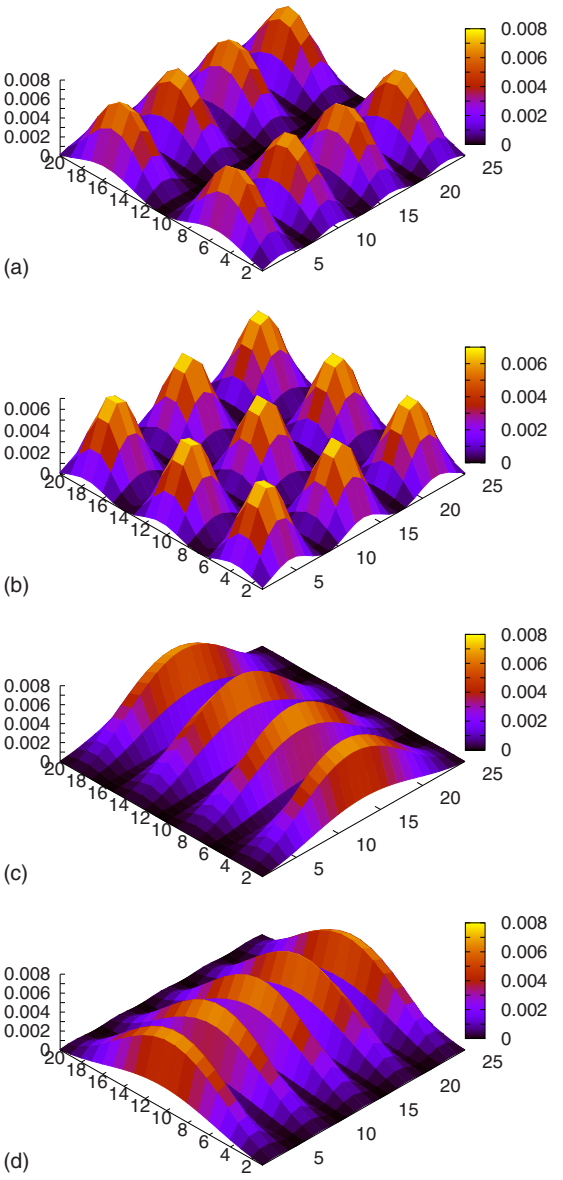

FIG. 1. (Color online) The localization probabilities associated to the four states included in the active window. $E_{10}=-3.68(k=1)$, $E_{11}=-3.67(k=2)$, $E_{12}=-3.63(k=3)$, and $E_{13}=-3.62(k=4)$ (in t_D units). The left lead is located near the lower left corner of the sample and the right lead coupled close to the upper right corner.

qualitatively the pulsed signal as given by the function $\chi_L(t)$ (arbitrary units are used on the corresponding axis). In the beginning the system is coupled to the leads and both contacts are kept open for a time t_0. Then the left contact is modulated by pulses while the other one is left open. The three signals do not drop at the same time because of the different shifts T_1 used in the construction of χ_L (we have $T_1=40.7$ ps, 44 ps, and 51.8 ps). As the sample dynamics adapts to the input signal a periodic regime is already established after two pulses. The first observation is that for very short pulses [$\tau_p=7.5$ ps in Fig. 2(a)] the output current J_R has a triangular shape although the modulating signal is rectangular. In addition J_R does not vanish when the left lead is disconnected, resembling the charging-relaxation character-

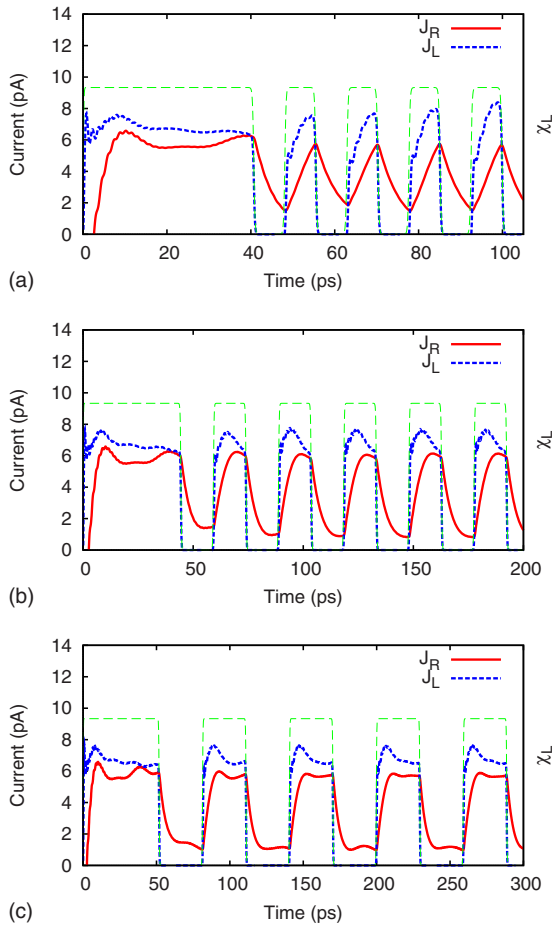

FIG. 2. (Color online) (a)–(c) Total currents in the input (left) and output (right) leads for the 25×20 sites system for different pulse lengths: (a) $\tau_p=7.5$ ps, (b) $\tau_p=15$ ps, and (c) $\tau_p=30$ ps. The bias window covers only two single-particle states. In Figs. 2(b) and 2(c) we show the currents for longer times than in Fig. 2(a) in order to capture the same number of pulses. The signal applied on the input contact is also qualitatively shown with a dashed line. The coupling strength $V_L=V_R=4$, $\mu_L=-3.65$, and $\mu_R=-3.7$.

istic of a capacitor. The charge is first absorbed from the left lead when the contact is switched on, and then only partially expelled into the right lead, when the contact to the left lead is off, i.e., even in the absence of a driving bias. The decay of the output signal looks exponential, but after one complete cycle, i.e., before the left contact opens again, the magnitude of the output current in the right lead is still considerable. The current in the left lead J_L decays much faster when the contact is turned off, following closer the modulation potential at the contacts. We notice that right after the left contact opens the current is injected in the sample quite fast but the current in the right lead increases slower.

When the pulse length increases the shape and the amplitude of the output current change considerably. J_R reaches maxima even before the pulse is turned off and remains almost constant during the second half of the pulse, while at the same time the input current decrease. However, at $\tau_p=15$ ps the output current still shows an exponential decay and does not reproduce the input signal. A different response to the pulse train is obtained at $\tau_p=30$ ps. In this case the output current decays first exponentially and then stays flat until the left contact opens again.

Comparing the behavior of the input currents in all three cases we see that in the first half of the 30 ps pulse the current is similar to the one that develops in the full length of the 15 ps pulse. The saw-tooth profile of the current in Fig. 2(a) is also present in the first half of the 15 ps pulse. This is due to the fact that as long as the sample is coupled to both leads it has the transient behavior which is already observed during the initial charging time. It is also clear that if the pulse length is too short the left lead does not feed enough charge to the sample in order to maintain a constant output current.

An estimate of the pulse length which generates an output current with almost a rectangular shape can be taken from the first transient period ($t<t_0$); that pulse length should be at least equal to the time at which the output current become nearly equal.

In Fig. 3(a) we compare the total charge accumulated on the two states within the bias window for the three pulse lengths. As the pulse length increases more charge is transferred through the system and therefore the output current increase. One should notice that for the 30 ps pulse the charge first relaxes exponentially but then almost linearly. Since the current is essentially the derivative of the charge with respect to time this means the current in the right lead is first exponential and then constant, as we have already learned from Fig. 2(c).

The knowledge of the reduced density operator provides also information on the charge density in each site i of the sample which is given by:

$$\langle Q_S(i,t)\rangle = \sum_{n,n'} \sum_{\nu,\nu'} \phi_n^*(i)\phi_{n'}(i)\rho_{\nu\nu'}(t)\langle\nu'|d_n^\dagger d_{n'}|\nu\rangle. \quad (8)$$

We present in Figs. 3(b) and 3(c) two snapshots of $\langle Q_S(i,t)\rangle$ for the configuration considered in Fig. 2(b). The charge distribution reflects the geometry of the two states within the bias window [see Figs. 1(a) and 1(b)] and provides interesting information on the electronic propagation in the system (note however that a "classical" picture of electrons' trajectory is not possible for the small system considered here). The electrons enter the sample from both leads and propagate mostly along the x axis. At later times $t=37$ ps a "snake"-like pattern of $\langle Q_S(i,t)\rangle$ emerges. We stress that the propagation along the "diagonal" of the sample is not guaranteed. Given the geometry of the second state [see Fig. 1(b)] it may very well happen that the charge is simply localized in that region, without a net flow toward the output lead.

We also find that when the contact to the left lead is closed the "snake" pattern is interrupted, which suggests that most of the charge crosses the sample along the edges, following the state shown in Fig. 1(a) (not shown).

In Figs. 4(a)–4(c) we show the currents obtained from the same sample when the chemical potential of the left lead is pushed to $\mu_L=-3.6$ and thus two more states enter into the bias window, i.e., those with $k=3$ and $k=4$. When comparing to Fig. 2 we observe additional "shoulders" developing in the output current. These shoulders are produced by the states

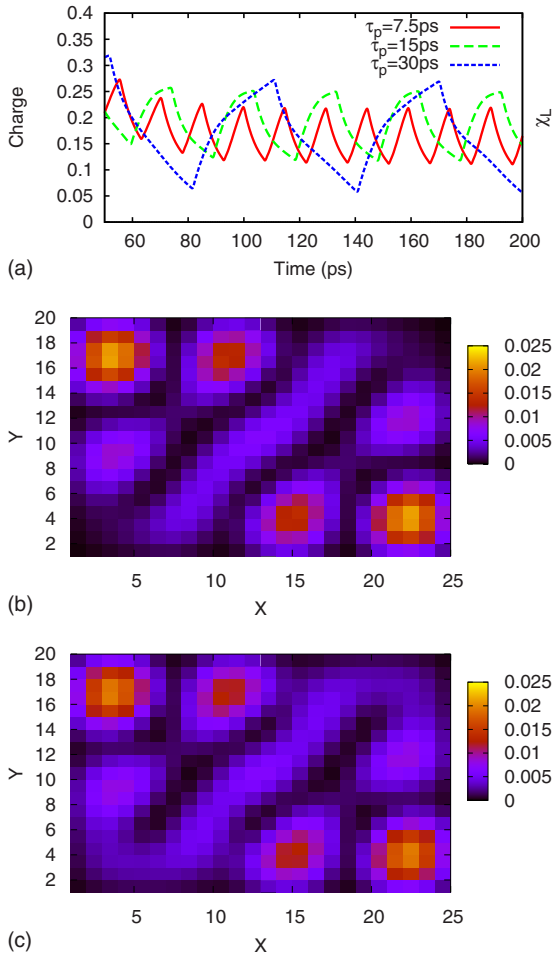

FIG. 3. (Color online) (a) The total charge accumulated on the two states from the bias window for the three pulse lengths considered in Figs. 2(a)–2(c). (b) and (c) The charge distribution $\langle Q_S(i,t)\rangle$ inside the sample at $t=1.48$ ps (b), and (c) $t=37$ ps. The pulse length is $\tau_p=15$ ps and the bias window covers only two single-particle states. At $t=37$ ps the coupling to the left lead is strong and a 'snake' contour appears. The coupling strength $V_L=V_R=4$, $\mu_L=-3.65$, and $\mu_R=-3.7$.

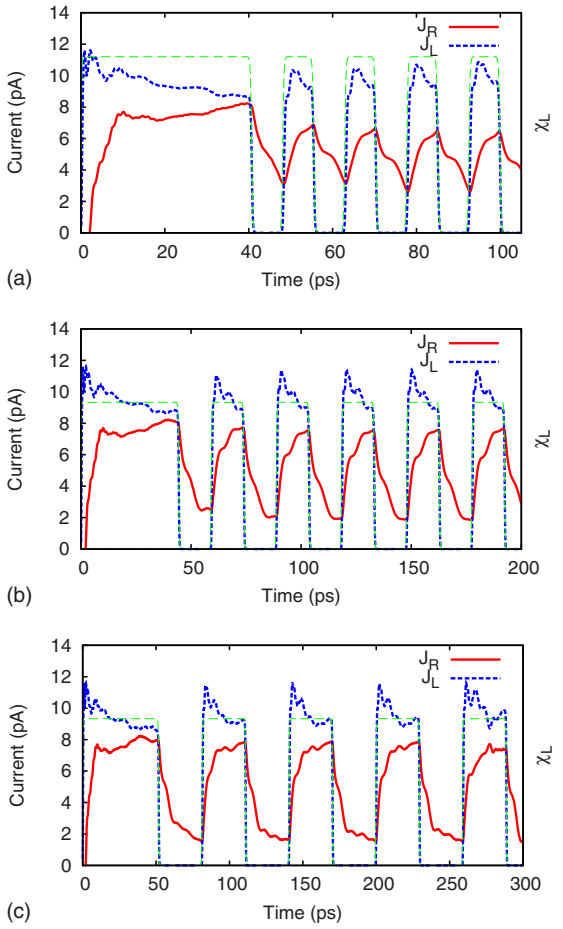

FIG. 4. (Color online) (a)–(c) Total currents in the input (left) and output (right) leads for the 25×20 sites system for different pulse lengths: (a) $\tau_p=7.5$ ps, (b) $\tau_p=15$ ps, and (c) $\tau_p=30$ ps. The bias window covers four single-particle states. The signal applied on the input contact is also given in arbitrary units-dashed line. The coupling strength $V_L=V_R=4$. $\mu_L=-3.6$, and $\mu_R=-3.7$.

included in the bias window during the relaxation into the right lead. The relaxation processes depend on the coupling between the states and the lead. Since one of the two states is only poorly coupled to the leads, i.e., the one with $k=3$ [see Fig. 1(c)], the shoulder is actually produced by the state with $k=4$.

In the following we compare the partial currents in the right lead for the two and four states configurations in the case of the ultrashort 7.5 ps pulse. The partial currents $J_{l,k}$ are calculated with Eq. (6). Figure 5(a) gives the output currents and confirms that the third state does not contribute significantly to the transport. Both $J_{R,1}$ and $J_{R,2}$ increase during the entire pulse length, although with a lower slope in the second part. Rather surprisingly, in this time interval $J_{R,4}$ decreases. In the relaxation interval the situation is the opposite: $J_{R,1}$ and $J_{R,2}$ are monotonously decreasing while the current of the fourth state considerably increases in the second half of the relaxation interval. The currents entering the sample from the left lead [see Fig. 5(b)] also have interesting features: $J_{L,1}$ and $J_{L,2}$ rise suddenly to a maximum value, while $J_{L,4}$ increases more slowly and does not reach a maximum within the pulse. This suggests that the two lowest states absorb quickly more charge from the left reservoir. By looking at the occupation numbers shown in Fig. 6(a) one convinces himself that this is indeed the case. The occupation of the fourth level increases much more slowly than N_1 and N_2.

The behavior of $J_{L,4}$ and $J_{R,4}$ can be explained by the dynamic tunneling processes described by the gain and loss terms of the solution of the master equation via the matrix Π_{ql}. Suppose, for example, that at time $s<t$ an electron tunnels from the input lead into the lowest state of the bias window, $k=1$. At instant t the same electron may tunnel out into the right lead. But it is also possible that this electron remains in the sample, while another electron, from another state, say the fourth, tunnels back into the left lead; escaping into the left lead from the fourth state is more likely than in the right lead because the chemical potential μ_L is much closer to E_{13} $(k=4)$ than μ_R. Repeated tunneling from highest state of the sample toward different leads and back into the sample lead to the charging of the lower states at the expense of the higher ones. Consequently the output currents

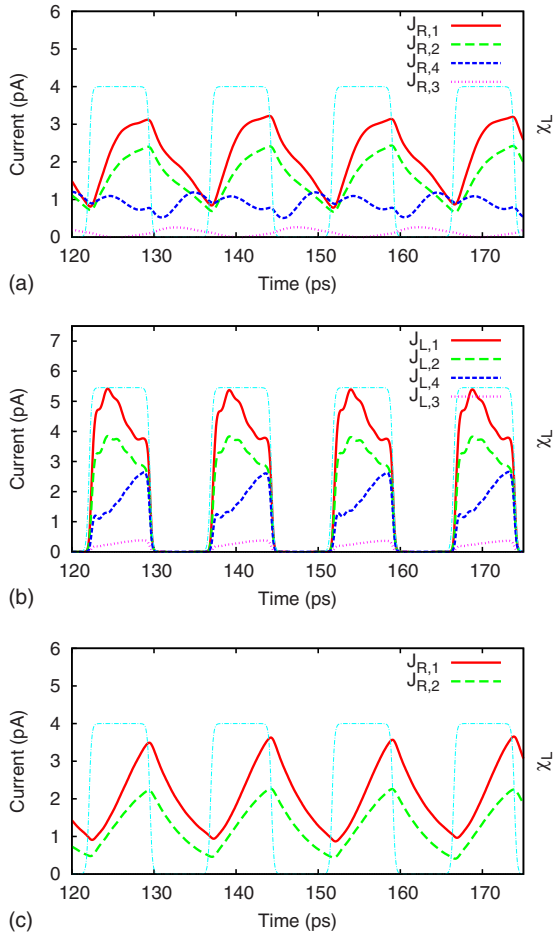

FIG. 5. (Color online) Partial currents in the output (a) and input (b) leads for the 25×20 sites system for $\tau_p=7.5$ ps, $\mu_L=-3.6$, and $\mu_R=-3.7$. In this case the bias window covers four states. (c) The output partial currents for the two-level configuration $\mu_L=-3.65$ and $\mu_R=-3.7$. The coupling strength is $V_L=V_R=4$.

associated to the lower states 1 and 2 are increasing, see Fig. 5(a), whereas the output current $J_{R,4}$ decreases. Note also that the net input current $J_{L,4}$ is smaller than $J_{L,1}$ and $J_{L,2}$ because there are more electrons tunneling out from the level $k=4$.

In contrast, when the pulse is turned off, the charge on the fourth level leaves the sample only via the output lead and therefore $J_{R,4}$ increases as shown in Fig. 5(a). On the other hand the tunneling processes from the left lead to the lowest levels are switched off and so $J_{R,1}$ and $J_{R,2}$ decrease on the relaxation interval.

For comparison we also show in Figs. 5(c) and 6(b) the output currents for the two-level configuration ($k=1,2$) and the occupation numbers. For the two-level configuration the partial occupation numbers display similar charging/relaxation shapes. This happens because these two particular states are equally coupled to the leads and hence the input signal propagates almost identically through both states toward the right lead. Remarkably, a similar behavior of the time-dependent occupation number was obtained from the experimental data by Lai *et al.*[4] In order to get more information on the relevant tunneling processes we have analyzed the diagonal elements (i.e., the populations) of the reduced

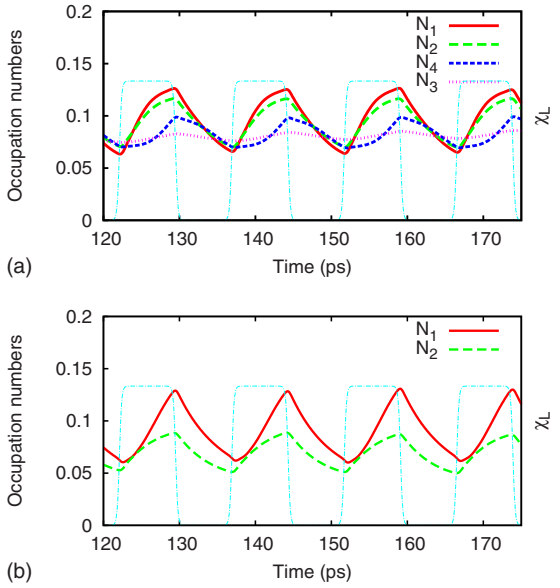

FIG. 6. (Color online) (a) The occupation numbers of states from the bias window for a pulse length $\tau_p=7.5$ ps, $\mu_L=-3.6$, and $\mu_R=-3.7$. (b) The same in the two-level case $\mu_L=-3.65$ and $\mu_R=-3.7$.

density operator. It useful to introduce a shorter notation for the many-body states by interpreting the occupation numbers as decimal numbers written as binary strings (but reading them in the reverse order, and adding 1). For example $|1\rangle=|0000\rangle$, $|2\rangle=|1000\rangle$, $|3\rangle=|0100\rangle$, etc.

Figure 7(a) shows the populations corresponding to the single-particle sector of the Fock space. We also give in Fig. 7(b) the most relevant two-particle configurations. The vacuum state $|0000\rangle$ has the largest probability ρ_{11} which is not shown. At $t=0$ it is 1 because the sample is initially empty, then during the charging period it drops to about 0.6, but it increases back to about 0.7 during the relaxation interval. From Fig. 7(a) we infer that (i) the configurations $|1000\rangle$ and $|0100\rangle$ are the most probable in the transient regime; (ii) the corresponding probabilities ρ_{22} and ρ_{33} decay exponentially (qualitatively speaking) during the relaxation, but ρ_{99} which is the probability of the state $|0001\rangle$ does not decay exponentially. This state is even stable for some time in the relaxation regime, while the probabilities for the states $|1000\rangle$ and $|0100\rangle$ decrease. This is another way of seeing that the 4th state relaxes later into the right lead. (iii) ρ_{55} is only slowly increasing and has only small oscillations due to the time-dependent signal, due to the weak coupling to the leads. The two-particle configurations shown in Fig. 7(b) have very small probability because the system is poorly charged during the ultrashort pulse considered here.

For completeness we give in Figs. 8(a)–8(c) the off-diagonal elements of the reduced density matrix, known as "coherences," which are related to the transitions between different states. For example ρ_{29} [Fig. 8(a)] describes the process in which electrons can tunnel from the 4th state into the leads and then back to the sample on the 1st state. We see that the real and imaginary parts of the coherences have oscillations and change sign. Moreover, the oscillations are more complex if the matrix element implies single-particle

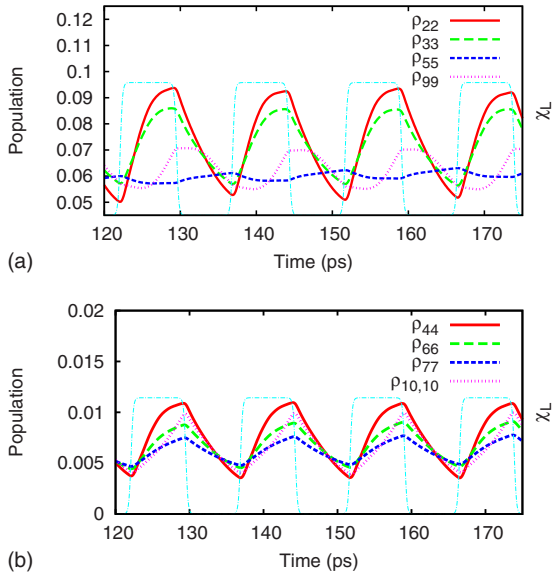

FIG. 7. (Color online) The relevant diagonal elements of the reduced density operator for the 25×20 sites system calculated with four single-particle states in the active region. (a) The diagonal elements of the reduced density operator corresponding to single-particle configurations $|2\rangle=|1000\rangle$, $|3\rangle=|0100\rangle$, $|5\rangle=|0010\rangle$, and $|9\rangle=|0001\rangle$. (b) The most relevant two-particle configurations $|4\rangle=|1100\rangle$, $|6\rangle=|1010\rangle$, $|7\rangle=|0110\rangle$, and $|10\rangle=|1001\rangle$. $\mu_L=-3.6$ and $\mu_L=-3.7$.

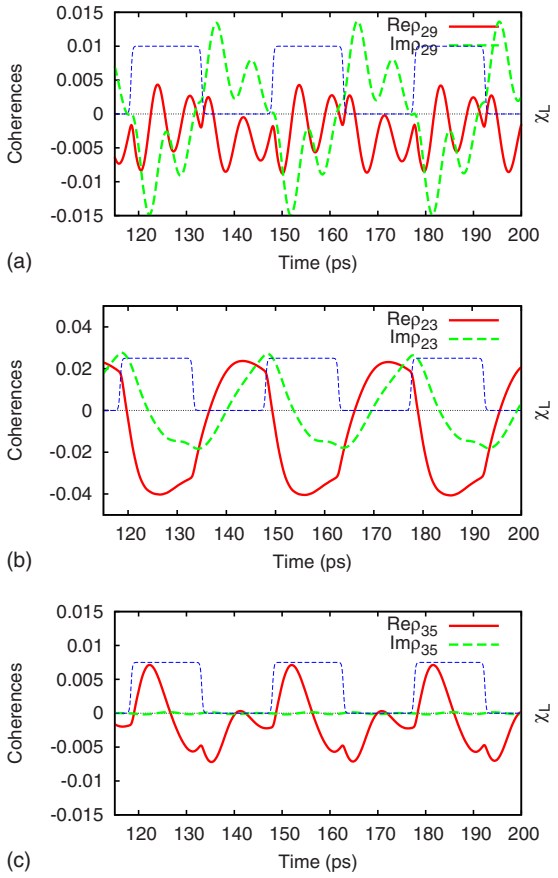

FIG. 8. (Color online) (a)–(c) The imaginary and real parts of the off-diagonal elements of the reduced density matrix which couple various states (see the discussion in the text). Note the multiple oscillations in any half period and the small amplitude for ρ_{29}. The dashed (blue) line represents the signal applied on the input contact. $\tau_p=15$ ps, $\mu_L=-3.6$, and $\mu_L=-3.7$.

states separated by other energy levels. Indeed, by comparing Re ρ_{23} and Re ρ_{29} we see that the latter displays two minima and two maxima in the charging time interval, while Re ρ_{23} has only one minimum. This feature suggests again that electrons make transitions via intermediate single-particle states as follows: initial state→intermediate state→leads→final state. We have checked that coherences between states with only one intermediate state in between (e.g., Re ρ_{39}) have only one maximum and one minimum.

Another remark is that the oscillations of ρ_{23} have a higher amplitude than the other two coherences, which is consistent to the fact that the two configurations $|2\rangle=|1000\rangle$ and $|3\rangle=|0100\rangle$ are the most probable ones in the stationary regime. Figure 8(c) shows that the third level is very weakly coupled to the level below, which is expected since that state is poorly coupled to the leads. By increasing the pulse width the number of oscillations during the pulse generally increases as more and more transitions may occur. Also, two-particle configurations will develop, while the probability of the single-particle states decrease (not shown). It should be mentioned here that in the non-Markovian approach the coherences also contribute to the currents because they are coupled to the diagonal elements of ρ.

An interesting question is whether there are other types of pulse that could be reproduced in the output current. We present in Figs. 9(a)–9(c) numerical results for triangular pulses applied to the same sample when only two states contribute to the transport (i.e., $\mu_L=-3.65$ and $\mu_R=-3.7$). We also used the same periods of the switching function χ_L in order to compare the results. The half width of the triangular pulse equals the length of the rectangular one. The relaxation characteristics are less obvious in this case because the coupling to the left lead increases and decreases linearly, not abruptly as before. The triangular shape of the pulse is rather well reproduced in the output current except for a slight asymmetry of its edges. The amplitude is also smaller.

We continue with similar results for a different sample, a narrow 40 nm$\times$160 nm quantum wire described by a $5\times20=100$ sites lattice. The system has now 100 eigenstates and it is connected to two three-channel leads on both narrow sides. For simplicity we consider uncoupled channels, which mean the electrons cannot jump between the channels. The chemical potentials of the leads are $\mu_L=-3$ and $\mu_R=-3.6$; they cover three states now, $E_3=-3.53$, $E_4=-3.38$, and $E_5=-3.19$ (or $k=1,2,3$ respectively) which we also consider as the active window. The coupling of these states to the leads is much stronger than in the previous case. Figure 10(a) shows the input/output characteristics for a pulse of length $\tau_p=7.5$ ps. We see that the total currents become equal in the second half of the pulse. This means that the stationary state is practically reached before the left contact is switched off. After that the output current is delayed with respect to the input current. This delay corresponds to the propagation of electrons along the sample. We have checked this by estimat-

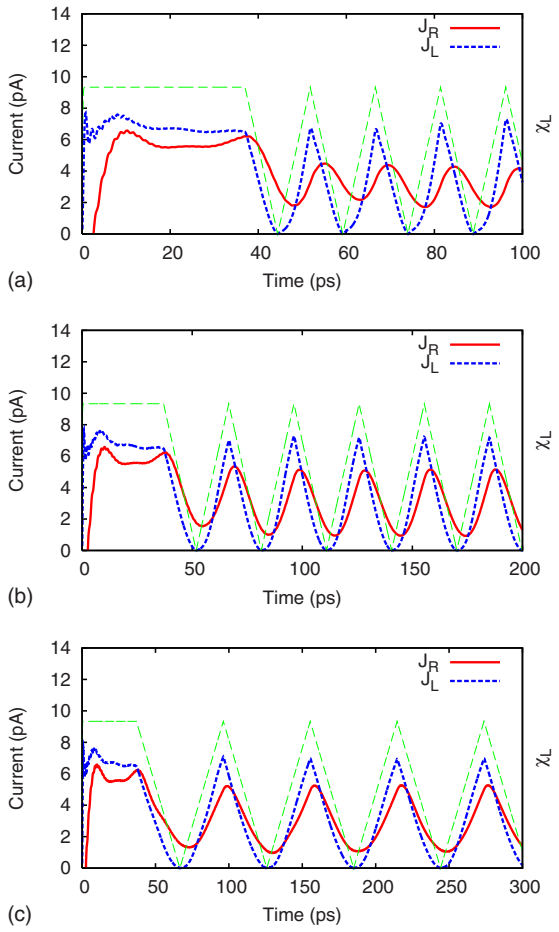

FIG. 9. (Color online) (a)–(c) Total currents in the input (left) and output (right) leads for the 25×20 sites system for triangular pulses of different half width: (a) $\tau_p=7.5$ ps, (b) $\tau_p=15$ ps, and (c) $\tau_p=30$ ps. The bias window covers only two single-particle states. The signal applied on the input contact is also qualitatively shown with a dashed line. The coupling strength $V_L=V_R=4$, $\mu_L=-3.65$, and $\mu_R=-3.7$.

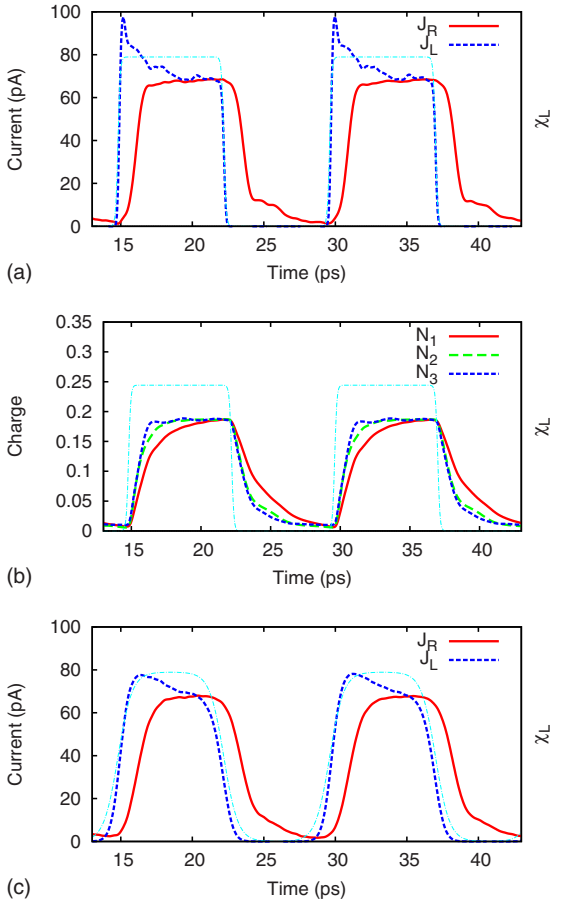

FIG. 10. (Color online) (a) The total input and output currents for a 5×20 sites system with three states within the bias window. J_R is delayed with respect to J_L. The pulse is rather squared [the dashed (green) line], with the rise time defined by the parameter $\gamma=1$. (b) The occupation numbers of the states within the bias window. Note that the lowest states relax at a slower rate due to a smaller coupling to the leads. (c) The total input and output currents for a smooth pulse ($\gamma=0.25$). $\tau_p=15$ ps, $\mu_L=-3$, and $\mu_L=-3.6$.

ing the time needed by one electron having the energy $E_4=2t_L\cos q$ to travel along the wire; we obtain that the traveling time is around 2 ps which agrees with the numerical results.

The input current has a sharp transient maximum as the left contact opens, but this behavior is not transferred to the output current which is rather flat. Again the relaxation input current has a 'step' after a fast decay. The occupation numbers of the three states within the bias window are shown in Fig. 10(b) and explain the origin of the step. The two higher states depopulate quite fast in the first half of the relaxation interval, but at some point their depletion suddenly slows down. This suggests that the relaxation rates are governed by time-dependent tunneling rates depending on the coupling to the leads, but also on the occupation number of the states. Remark that the bias window becomes empty before another pulse rises up.

The rise time of the pulse can be varied in experiments (see Ref. 3). In our model the rise time depends on the smoothness parameter γ used to create the pulses. In Fig. 10(c) we show the total input and output currents for a pulse with a larger rise time corresponding to $\gamma=0.25$. The transient maxima in the input current soften and so does the additional shoulder in the relaxation current. Note however that during the pulse the output current takes the same value (around 60 pA) and it is still delayed with respect to the input current.

Finally we would like to comment on the Coulomb interaction which is neglected here. The numerical results show that the occupation number of the levels within the active window is quite low for the rather large samples considered [see, e.g., Figs. 6(a) and 6(b)]. In this case one expects that the Coulomb interaction between electrons located in the active states causes very small changes in the transient currents. On the other hand, the Coulomb repulsion generated by the inactive states which are fully occupied could be important, leading at least to a Hartree shift of the active levels. However, the relaxation processes and the modulation of the output current should be qualitatively similar.

IV. CONCLUSIONS

We have analyzed the transient response of a two-dimensional nanosystem to a sequence of periodic rectangular pulses which modulate the contact to the source lead. By solving the generalized non-Markovian master equation for the reduced density matrix we have been able to discuss the dependence of the input/output characteristics on the pulse length for two specific systems: a rather large quantum dot and a narrow quantum wire. We have considered a pump-and-probe setup in which the contact to the left lead opens and closes periodically while the right lead is always connected to the system. When the contact is switched off the drain current reflects the relaxation processes in the sample. We have discussed these processes by analyzing the single-particle currents, diagonal, and off-diagonal elements of the reduced density matrix. At a low temperature the phonon effects could be neglected and the main relaxation processes are back-and-forth tunnelings to and from the leads.

In both cases (the dot and the wire) we have found that the pulse length can be adjusted such that the shape of the pulse can be reproduced by the output signal. By increasing the chemical potential of the source lead the current profile in the output lead develops additional oscillations related to the relaxation of the higher-energy states included in the bias window. In the case of a narrow quantum wire a delay of the output current with respect to the input signal has been obtained.

This study was partly motivated by the recent experiments of Naser *et al.*[3] and Lai *et al.*[4] Although those experiments were done with larger and longer pulses our results qualitatively agree with the reported features of the transient response. In particular the time-dependent occupation number clearly show a charging/relaxation behavior as in the work of Lai *et al.*[4]

ACKNOWLEDGMENTS

This work was supported by the Icelandic Science and Technology Research Program for Postgenomic Biomedicine, Nanoscience, and Nanotechnology; the Computing Center for Design of Materials and Devices, Icelandic Research Fund Grant No. 090025011; the Research Fund of the University of Iceland; and the Development Fund of the Reykjavik University Grant No. T09001. V.M also acknowledges the hospitality of the Science Institute and the partial financial support from PNCDI2 program (Grant No. 515/2009) and Grant No. 45N/2009.

[1] T. Fujisawa, T. Hayashi, and S. Sasaki, Rep. Prog. Phys. **69**, 759 (2006).
[2] R. Hanson, L. P. Kouwenhoven, J. R. Petta, S. Tarucha, and L. M. Vandersypen, Rev. Mod. Phys. **79**, 1217 (2007).
[3] B. Naser, D. K. Ferry, J. Heeren, J. L. Reno, and J. P. Bird, Appl. Phys. Lett. **89**, 083103 (2006); **90**, 043103 (2007).
[4] W.-T. Lai, D. M. T. Kuo, and P.-W. Li, Physica E **41**, 886 (2009).
[5] G. Stefanucci and C.-O. Almbladh, Phys. Rev. B **69**, 195318 (2004).
[6] S. Kurth, G. Stefanucci, C.-O. Almbladh, A. Rubio, and E. K. U. Gross, Phys. Rev. B **72**, 035308 (2005).
[7] V. Moldoveanu, V. Gudmundsson, and A. Manolescu, Phys. Rev. B **76**, 085330 (2007).
[8] V. Gudmundsson, G. Thorgilsson, C.-S. Tang, and V. Moldoveanu, Phys. Rev. B **77**, 035329 (2008).
[9] M. Switkes, C. M. Marcus, K. Campman, and A. C. Gossard, Science **283**, 1905 (1999).
[10] L. Arrachea, Phys. Rev. B **72**, 125349 (2005).
[11] J. Splettstoesser, M. Governale, J. König, and R. Fazio, Phys. Rev. B **74**, 085305 (2006).
[12] G. Stefanucci, S. Kurth, A. Rubio, and E. K. U. Gross, Phys. Rev. B **77**, 075339 (2008).
[13] J. H. Oh, D. Ahn, and S. W. Hwang, Phys. Rev. B **71**, 205321 (2005).
[14] V. Moldoveanu, V. Gudmundsson, and A. Manolescu, N. J. Phys. **11**, 073019 (2009).
[15] S. Nakajima, Prog. Theor. Phys. **20**, 948 (1958).
[16] R. Zwanzig, J. Chem. Phys. **33**, 1338 (1960); Lect. Theor. Phys. **3**, 106 (1960).
[17] I. Prigonine and P. Resibois, Physica (Amsterdam) **27**, 629 (1961).
[18] U. Harbola, M. Esposito, and S. Mukamel, Phys. Rev. B **76**, 085408 (2007).
[19] X.-Q. Li, J. Luo, Y.-G. Yang, P. Cui, and Y. J. Yan, Phys. Rev. B **71**, 205304 (2005).
[20] E. Vaz and J. Kyriakidis, J. Phys.: Conf. Ser. **107**, 012012 (2008).
[21] J. Rammer, A. L. Shelankov, and J. Wabnig, Phys. Rev. B **70**, 115327 (2004).
[22] A. Braggio, J. König, and R. Fazio, Phys. Rev. Lett. **96**, 026805 (2006).
[23] D. Urban, J. König, and R. Fazio, Phys. Rev. B **78**, 075318 (2008).
[24] S. Welack, M. Schreiber, and U. Kleinekathöfer, J. Chem. Phys. **124**, 044712 (2006).
[25] U. Kleinekathöfer, G. Q. Li, S. Welack, and M. Schreiber, Europhys. Lett. **75**, 139 (2006); G. Q. Li, S. Welack, M. Schreiber, and U. Kleinekathöfer, Phys. Rev. B **77**, 075321 (2008).
[26] V. Gudmundsson, C. Gainar, C.-S. Tang, V. Moldoveanu, and A. Manolescu, New J. Phys. **11**, 113007 (2009).
[27] J. B. Maddox, U. Harbola, N. Liu, C. Silien, W. Ho, G. C. Bazan, and S. Mukamel, J. Phys. Chem. A **110**, 6329 (2006).
[28] F. Haake, *Statistical Treatment of Open Systems by Generalized Master Equations*, Springer Tracts in Modern Physics Vol. 66 (Springer, Berlin, 1973) p. 98.
[29] C. Timm, Phys. Rev. B **77**, 195416 (2008).
[30] A.-P. Jauho, N. S. Wingreen, and Y. Meir, Phys. Rev. B **50**, 5528 (1994).